Published June 29, 2009

Biogenesis of cytochrome b_6 in photosynthetic membranes

Denis Saint-Marcoux,[1,2] Francis-André Wollman,[1,2] and Catherine de Vitry[1,2]

[1]Centre National de la Recherche Scientifique, UMR 7141, Physiologie Membranaire et Moléculaire du Chloroplaste, Institut de Biologie Physico-Chimique, 75005 Paris, France
[2]Université Pierre et Marie Curie, Paris Universitas 06, UMR 7141, 75005 Paris, France

In chloroplasts, binding of a *c*′-heme to cytochrome b_6 on the stromal side of the thylakoid membranes requires a specific mechanism distinct from the one at work for *c*-heme binding to cytochromes *f* and c_6 on the lumenal side of membranes. Here, we show that the major protein components of this pathway, the CCBs, are bona fide transmembrane proteins. We demonstrate their association in a series of hetero-oligomeric complexes, some of which interact transiently with cytochrome b_6 in the process of heme delivery to the apoprotein. In addition, we provide preliminary evidence for functional assembly of cytochrome b_6f complexes even in the absence of *c*′-heme binding to cytochrome b_6. Finally, we present a sequential model for apo- to holo-cytochrome b_6 maturation integrated within the assembly pathway of b_6f complexes in the thylakoid membranes.

Introduction

Heme (Fe-protoporphyrin IX) is an essential cofactor for many fundamental biological processes. It is a hydrophobic and cytotoxic macrocycle, which therefore requires specific pathways to be safely delivered to its subcellular destinations. The *c*-type cytochromes (cyts) are most frequently characterized by the covalent attachment of heme to the protein by two thioether bonds formed between the heme vinyl groups and the thiols of two cysteines in a conserved CXXCH motif, with histidine as one of the axial ligands to the heme iron. Binding of *c*-heme comprises several critical steps including the reduction of cysteine residues, ferrous heme-supply, and heme-binding by itself. Factors involved in covalent heme binding have been extensively studied in prokaryotes and eukaryotes, and this maturation process usually occurs through one of three multifactorial systems (I, II, and III), depending on the biological organism and cellular compartment that are known to operate on the positive side (*p* side) of the membrane facing the periplasmic/intermembrane/lumenal space (Kranz et al., 1998; Thöny-Meyer, 2002; Allen et al., 2008; Ferguson et al., 2008; Giege et al., 2008; Hamel et al., 2009). It has been recently recognized that there are in fact two independent *c*-heme maturation pathways in the chloroplast: system II, also referred to as cyt *c* synthesis (CCS) on the *p* side of membranes (Xie and Merchant, 1996; Inoue et al., 1997); and the newly characterized system IV, also referred to as cofactor assembly on complex C subunit B (CCB) on the negative side (*n* side) of photosynthetic membranes facing the chloroplast stroma or cyanobacterial cytoplasm (Kuras et al., 2007).

Cyt *bc* complexes that associate *c*-type hemes, *b*-type hemes, and iron–sulfur centers are ubiquitous in energy-transducing membranes, where they transfer electrons from a lipid-soluble carrier to a water-soluble protein carrier, while building up a transmembrane proton gradient. Although quite similar to the bc_1 complex, its homologue found in bacteria and mitochondria, the b_6f complex contains additional cofactors. Six years ago, the discovery of an additional heme bound to the protein backbone of cyt b_6 (Kurisu et al., 2003; Stroebel et al., 2003) came as a major surprise. This new *c*-heme showed unusual features. It is covalently attached by a unique thioether bond to the conserved Cys-35 of the b_6 subunit (*Chlamydomonas reinhardtii* numbering), and thus belongs to the *c*-type family. It is a high spin *c*′-heme, with a pentacoordinated central iron. The usual amino acid axial ligands of the heme iron are missing, but a water molecule (or hydroxide ion) acts as a unique axial ligand and bridges the heme iron to a propionate side chain of b_H-heme. Furthermore, c_i-heme is attached on the membrane

Correspondence to Catherine de Vitry: catherine.devitry@ibpc.fr

Abbreviations used in this paper: BN, blue native; CCB, cofactor assembly on complex C subunit B; Ccm, cytochrome *c* maturation; CCS, cytochrome *c* synthesis; cyt, cytochrome; *n* side, negative side; OEE, oxygen evolution enhancer; PS, photosystem; *p* side, positive side; TMD, transmembrane domain; WT, wild type.

The Rockefeller University Press $30.00
J. Cell Biol. Vol. 185 No. 7 1195–1207
www.jcb.org/cgi/doi/10.1083/jcb.200812025

Published June 29, 2009

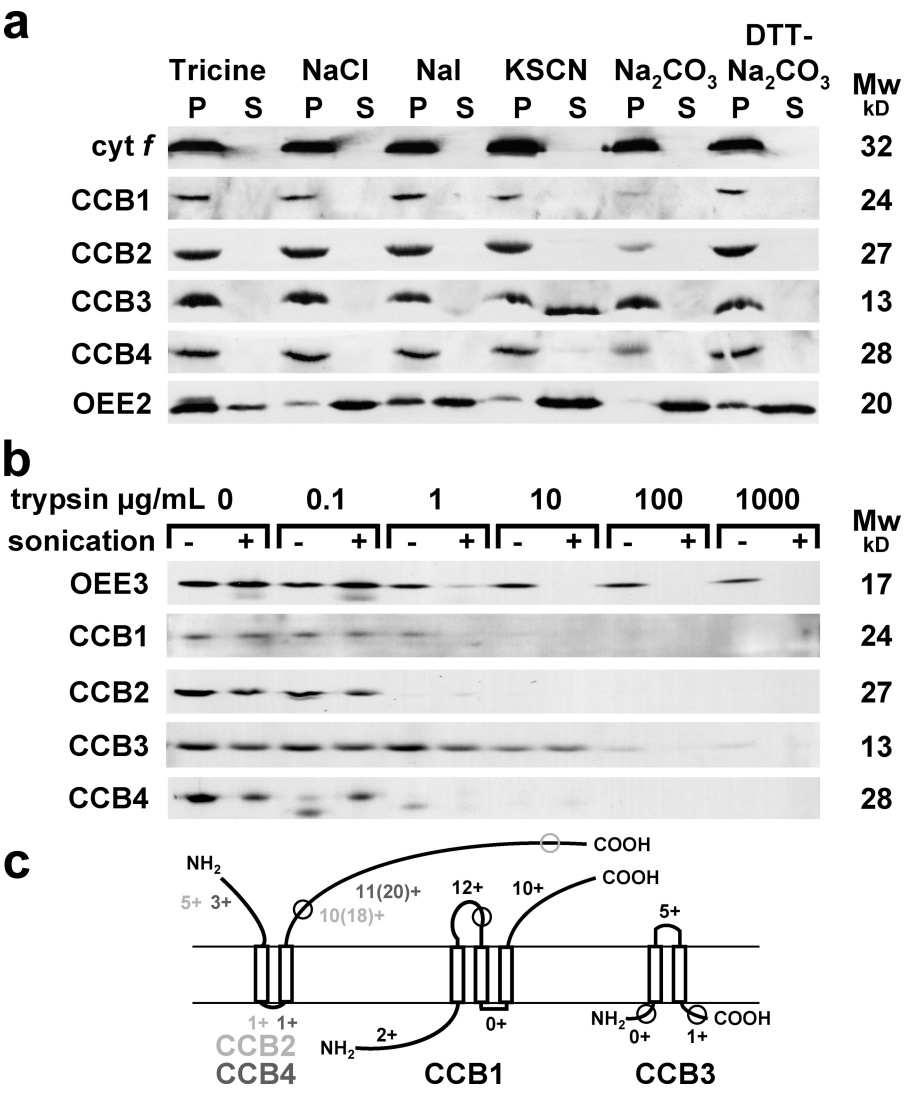

Figure 1. **Transmembrane topology analysis of CCBs.** Samples were separated by SDS-PAGE and analyzed by ECL immunodetection with antipeptide antibodies against CCB1, CCB2, CCB3, and CCB4; and with antisera against intrinsic cyt *f*, extrinsic OEE2, and OEE3 PSII subunits. (a) Extraction of membrane proteins by dissociating treatments. Membranes were frozen and thawed twice in the indicated solutions: 20 mM tricine-NaOH buffer, pH 8.0 (Tricine), 2 M NaCl in 20 mM tricine-NaOH buffer, pH 8.0 (NaCl), 1.5 M NaI in 20 mM tricine-NaOH buffer, pH 8.0 (NaI), 2 M KSCN in 20 mM tricine-NaOH buffer, pH 8.0 (KSCN), 0.1 M Na_2CO_3 (Na_2CO_3), and 0.1 M Na_2CO_3 + 0.1 M DTT (DTT-Na_2CO_3). The supernatant and the pellet were recovered after a 100,000-*g* centrifugation. The pellet was extracted a second time using an identical procedure. The first supernatant (S) and the second pellet (P) were analyzed. (b) Proteolysis of membrane vesicles. Membrane vesicles were incubated for 30 min with increasing trypsin protease concentrations (an endoproteinase cutting after positively charged residues in Lys-C and Arg-C) and sonicated (+) or not sonicated (−). (c) Schematized transmembrane topology predicted by sequence analysis and consistent with chaotrope extraction, protease accessibility, and split ubiquitin data. The numbers of positively charged residues after the positive inside rule are indicated for predicted mature protein when a different total number of positively charged residues is also indicated in parenthesis. Antipeptide localizations are circled.

n side in the quinone-binding pocket Q_i in very close proximity to b_H-heme, opposite to the location of *f*-heme and c_6-heme that are on the membrane *p* side.

Our previous genetic studies in *C. reinhardti* led to the identification of four nuclear *CCB* loci that control the process of apo- to holo-cyt b_6 conversion that involves binding of c_i-heme (Gumpel et al., 1995; Kuras et al., 1997, 2007; de Vitry et al., 2004). The signature of cyt b_6 impaired in c_i-heme binding was characterized in the *petB-C35V* mutant (the *petB* gene codes for cyt b_6), where the unique covalent cysteine ligand to the heme was substituted by a valine (de Vitry et al., 2004). It consists of a double band on urea-SDS-polyacrylamide gels or a single band of lower apparent molecular mass than in the wild type (WT) on SDS-polyacrylamide gels that shows no peroxidase activity. The same signature is observed in all *ccb* mutants, which indicates that they do not undergo binding of c_i-heme to cyt b_6. This entirely new biogenesis pathway comprises at least the four CCB factors, which are present in all photosynthetic organisms containing b_6f complexes (available under GenBank/EMBL/DDBJ accession nos. EF190472, EF190473, EF190474, and EF190475), for which no function had been previously ascribed (Kuras et al., 2007). CCB1 is ubiquitous among organisms performing oxygenic photosynthesis, where it is present as a unique orthologue. CCB3, which is the most conserved member of the CCB pathway, belongs to the large YGGT protein family (InterPro accession no. IPR003425) found in both plastids and bacteria. CCB2 and CCB4 are encoded by paralogue genes in *C. reinhardtii* with a low similarity level and derived from a unique cyanobacterial ancestor. We recently demonstrated the conserved function of the CCBs in *Arabidopsis thaliana* chloroplasts, where they are also involved in c_i-heme binding to cyt b_6 (Lezhneva et al., 2008).

Here, using *C. reinhardtii* as an experimental system for the investigation of the CCB maturation pathway, we extended our previous biochemical work that established the chloroplast membrane localization of CCBs (Kuras et al., 2007). We examined the topology and interactions between the CCBs as well as with cyt b_6 and demonstrate that the CCB pathway is organized within the thylakoid membrane in a series of distinct protein complexes that control the covalent binding of c_i-heme to cyt b_6.

Published June 29, 2009

Results

CCBs are transmembrane proteins that resist extraction with chaotropic agents

In our previous work, the CCB1–4 proteins were immunodetected as chloroplast membrane proteins after subcellular fractionation in *C. reinhardtii* (Kuras et al., 2007). Using fluorescent protein reporters, we also demonstrated that the CCB1–4 proteins are targeted to the chloroplast in *A. thaliana* (Lezhneva et al., 2008).

We further analyzed the transmembrane topologies of these proteins in *C. reinhardtii* by membrane treatment with chaotropic agents and by subjecting oriented thylakoid membranes vesicles to protease treatments followed by urea/SDS-PAGE and immunodetection with anti-CCB peptide antibodies. When membranes were treated with various chaotropic agents or incubated at high ionic strength or alkaline pH, a typical peripheral membrane polypeptide (oxygen evolution enhancer 2 protein of photosystem [PS] II [OEE2]) was released in the supernatant (Fig. 1 a). In contrast, cyt *f* was not extracted by these treatments, as expected from its transmembrane domain (TMD). All CCB factors behaved as bona fide transmembrane proteins. Although CCB3 resisted extraction at high ionic strength and alkaline pH, we noted that some CCB3 dissociated from the membrane with the chaotropic agent KSCN, which is intriguing for such a highly hydrophobic protein.

The transmembrane topology of the CCBs was assessed by protease treatment of French press–derived membrane vesicles. Membrane vesicles subjected or not subjected to sonication were incubated in the presence of trypsin (Fig. 1 b). Before sonication, most of the thylakoid vesicles were in a right-side-out orientation, and exogenous proteases have no access to their lumenal side. In contrast, upon sonication, the vesicles burst, and exogenous proteases gain access to both sides of the membranes. Typically, the PSII subunit OEE3, used here as a control for peripheral proteins on the lumenal side of the membranes, is degraded only after sonication, when using trypsin concentrations below 10 µg/ml. In contrast, CCB1, CCB2, and CCB4 proteins are degraded by trypsin treatments below 10 µg/ml even in the absence of sonication. Only CCB3 required higher trypsin concentration (100 µg/ml) for degradation, confirming its deep embedment in the membrane. The lumenal localization of the C terminus of CCB3 was supported by the lack of detection of a CCB3 digestion product corresponding to the mature protein missing the three C-terminal amino acid residues. Therefore, we conclude that the four CCB factors have stromal-exposed segments containing Lys and Arg residues as schematized in the transmembrane topology of the CCBs in Fig. 1 c (which also shows the localization of the epitopes against which our antibodies were prepared).

Concerted accumulation of CCB2 and CCB4 in *ccb* mutants

Each of the CCBs—CCB1 (24 kD), CCB2 (27 kD), CCB3 (13 kD), and CCB4 (28 kD)—is absent in the corresponding *ccb* mutant (Kuras et al., 2007). In a first attempt to identify possible interactions between CCB factors, we wondered whether the absence of one CCB factor in the corresponding *ccb* mutant would alter the accumulation pattern of the other CCBs. CCB1 and CCB3 accumulated to the WT level, independently of the presence or absence of the other CCBs (Fig. 2). The accumulation of CCB2 and CCB4 was similar in WT, *ccb1*, and *ccb3* mutants, and therefore independent of CCB1 and CCB3 accumulation (Fig. 2). However, CCB4 was barely detectable in the *ccb2* mutant, and, conversely, CCB2 was barely detectable in the *ccb4* mutant (Fig. 2). Thus, CCB2 and CCB4 show a concerted accumulation that suggests they form a heterodimer. We then looked at whether the presence of cyt b_6, as a substrate for c_i-heme binding, controlled the accumulation of the CCBs. We observed that the four CCBs still accumulated to the WT level in a mutant lacking cyt b_6 (*ΔpetB*) or in the *petB-C35V* mutant that bears a point mutation in the sequence of cyt b_6 that prevents c_i-heme binding (Fig. 2; de Vitry et al., 2004).

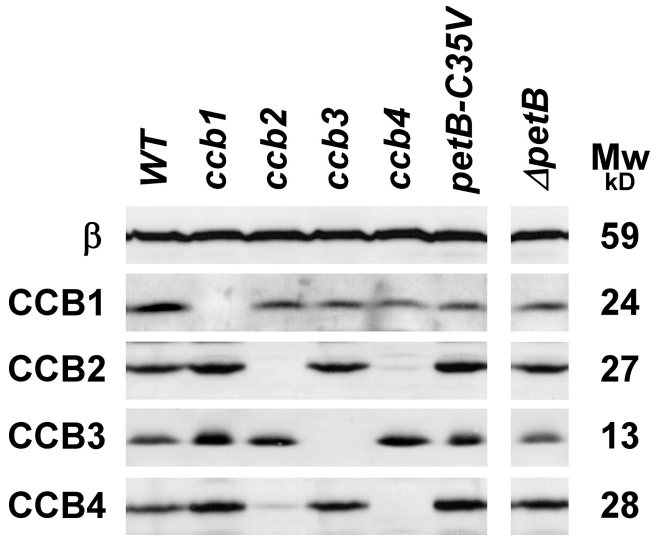

Figure 2. **Immunodetection of CCBs in WT and mutant cells.** *ccb* strains: nuclear mutants affecting specifically binding of c_i-heme to cyt b_6. *petB-C35V* strain: site-directed mutant of the chloroplast *petB* gene encoding cyt b_6 with a substitution of Cys35 preventing thioether bonding of c_i-heme to cyt b_6. *ΔpetB* strain: *petB* deletion strain. Whole cell proteins were separated by SDS-PAGE and analyzed by immunoblotting. A subunit of mitochondrial ATP synthase was immunodetected as a loading control (β).

Direct interaction of CCB2 and CCB4 in yeast split ubiquitin two-hybrid assays

We further investigated CCB2–CCB4 interactions using the yeast split ubiquitin system that is appropriate for testing interactions between two transmembrane proteins (as chloroplast membrane proteins [Pasch et al., 2005] and components of the cyt *c* maturation system I [Rayapuram et al., 2008]). Their interaction allows reconstitution of an active ubiquitin from its N and C terminus domains (Nub and Cub), fused, respectively, to each protein. The restored ubiquitin activity cleaves a transcription factor fused to Cub, thereby releasing auxotrophy for some particular nutrients.

Yeast cotransformed with CCB2 and CCB4 were able to grow on a very stringent medium for two reciprocal couples, either CCB2 fused to NubG with CCB4 fused to Cub

Published June 29, 2009

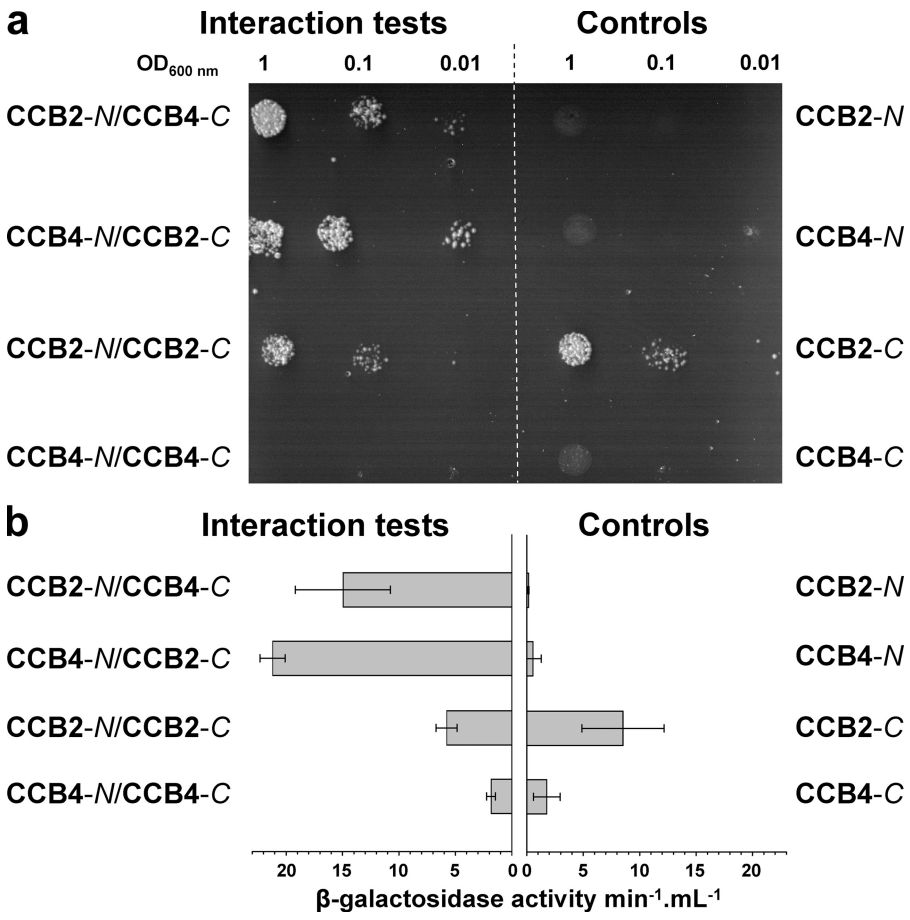

Figure 3. **CCB2 and CCB4 interaction in a yeast split ubiquitin two-hybrid assay.** Constructs CCB2-N or 4-N expressing CCB2 (or 4) mature protein fused to the mutated N-terminal half of ubiquitin NubG were cotransformed in yeast with constructs CCB2- (or 4)-C expressing CCB2 (or 4) protein fused the C-terminal half of ubiquitin Cub; tests of these protein interactions are shown on the left side of the broken line. Constructs expressing yeast protein Alg5, not expected to interact with CCBs, fused to Cub or NubG, were cotransformed, respectively with the CCB2- (or 4)-N or CCB2- (or 4)-C constructs; results of these controls are shown on the right side of the broken line. The interaction between two proteins at the membrane of yeast allows ubiquitin reconstitution and results in the activation of auxotrophic growth markers *ADE2* and *HIS3* and reporter gene *lacZ*. (a) To monitor expression of auxotrophic growth markers *ADE2* and *HIS3*, several cotransformant clones were resuspended in water to an OD_{600nm} of 1, 0.1, and 0.01; plated on SD medium lacking leucine, tryptophan, histidine, and adenine with 10 mM 3-aminotriazole; and allowed to grow for 30 h. (b) Expression of *lacZ* was followed by measuring at OD_{417nm} the accumulation of the product metabolized by β-galactosidase. Liquid SD medium lacking leucine and tryptophan was inoculated with several cotransformant clones, and cultures were allowed to grow for 16 h. After cell lysis, β-galactosidase activity was measured as described in Materials and methods and quantified according to the following formula: Activity = $1{,}000 \times DO_{417nm}/V \times t \times DO_{600nm}$, were V is the volume of assay and t is the time of incubation. All assays were repeated three times and the resulting error bars are shown.

(CCB2-N/CCB4-C) or CCB4 fused to NubG with CCB2 fused to Cub (CCB4-N/CCB2-C; Fig. 3 a). The interaction between CCB2 and CCB4 was confirmed by β-galactosidase activity assays (Fig. 3 b). The strength of the interaction between CCB2 and CCB4 was similar for the two reciprocal sets of constructs. In contrast, CCB2 fused both to NubG and to Cub or CCB4 fused both to NubG and to Cub (respectively, CCB2-N/CCB2-C and CCB4-N/CCB4-C) did not allow better growth than observed in control strains (yeast cotransformed with noninteracting Alg5 fused to NubG or Cub). These results argue for hetero-oligomerization of CCB2 with CCB4 with no homo-interaction between two copies of CCB2 or of CCB4. We could not find any evidence for a hetero-oligomerization between separate domains of CCB2 and CCB4, whether we tested soluble or TMDs of each protein (not depicted). With this technique, we also found no evidence for an interaction between CCB1 and CCB2 or CCB4 (not depicted). Finally, no interactions between any of these three CCBs and cyt b_6 could be detected in split ubiquitin assays (unpublished data). We note, however, that a positive control for the expression of CCB1, using cotransformation of the C terminus of CCB1 fused to Cub and Alg5 fused to NubI, further supported the localization of the C terminus of CCB1 in the cytosol (not depicted). The transmembrane configuration of CCB3 with its N and C termini in the lumen prevented us from studying CCB3 interactions in the split ubiquitin system, which requires an N or C terminus of the protein of interest to be present in the yeast cytoplasm.

CCB complexes analyzed on blue native (BN)-PAGE

To get a broader picture of the variety of membrane protein complexes that may contain CCBs, we separated oligomeric proteins on BN-PAGE, after a mild digitonin solubilization of thylakoid membranes, using a procedure similar to the one that has been developed for membrane protein complexes from mitochondria (Schägger and von Jagow, 1991; Meyer et al., 2005) and from chloroplasts (Lennartz et al., 2006). The constitutive subunits of the oligomers were separated in a second dimension on SDS-PAGE, followed by immunoblotting with antibodies raised against each CCB or against some of the major b_6f complex subunits. Fig. 4 compares BN-PAGE assays in the WT and in a series of mutant strains defective for c_i-heme binding to cyt b_6. In agreement with the concerted accumulation and split ubiquitin experiments that demonstrated extensive interactions between CCB2 and CCB4, we observed that these two CCB components comigrate at 70 kD by BN-PAGE (Fig. 4, circles) in all strains except in the *ccb2* mutant (Fig. 4) and *ccb4* mutant (not depicted), which lack these two proteins. Therefore, we attribute this 70-kD complex to the CCB2/CCB4 heterodimer. Monomeric forms of CCB2 and CCB4 that probably result from dissociation of the heterodimer were also detected in these experiments, with an apparent molecular mass of ~45 kD and 50 kD, respectively.

Among the various c_i-heme–binding mutants that we assayed in BN-PAGE, the *petB-C35V* mutant, which is specifically

Published June 29, 2009

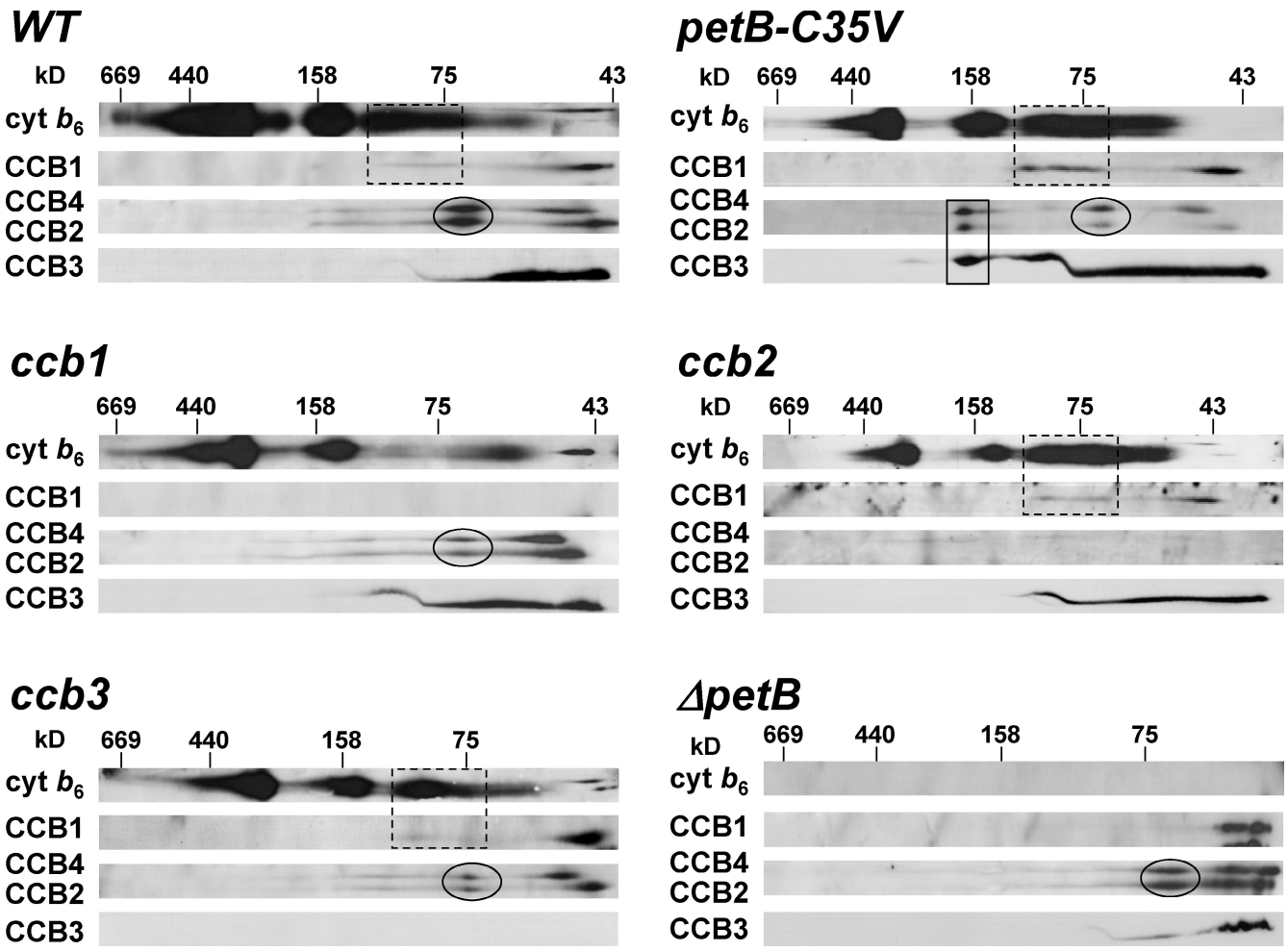

Figure 4. **CCB complexes after BN-PAGE of digitonin-solubilized membranes.** Same strains are shown as in Fig. 2. Digitonin-solubilized proteins were separated in the first dimension by BN-PAGE and in the second dimension by SDS-PAGE, and analyzed by ECL immunodetection. The positions of the molecular weight markers are indicated: thyroglobulin, 669 kD; ferritin, 440 kD; aldolase, 158 kD; conalbumin, 75 kD; and ovalbumin, 43 kD. The CCB2/CCB4 heterodimer is circled. CCB2/CCB4/CCB3 comigration is indicated by a solid box. CCB1/b_6 comigration is indicated by dashed boxes. Cyt b_6 was immunodetected after deprobing α-CCB1 immunodetection, and therefore shows residual detection of CCB1 and cross-reactant below CCB1.

blocked at the last stage of the binding process due to the replacement of the cysteine covalent ligand of the heme by an inactive valine, is the only one that has the same CCB complement as in the WT. A conspicuous feature of the immunodetection pattern in *petB-C35V* is the increased detection of several CCB-containing oligomers that were present only in trace amounts in the WT. This applies to oligomeric forms of CCB1 in the 70–110 kD region (Fig. 4, dashed boxes) and to oligomeric forms of CCB2/4/3 around 170 kD (Fig. 4, solid boxes). These observations suggest that these protein complexes are transiently formed in the process of heme delivery to cyt b_6 in the WT but accumulate more extensively in the *petB-C35V* mutant because the last step of heme binding is impaired. The CCB1-containing oligomer at 70–110 kD remained visible in *ccb2*, *ccb4*, and *ccb3* mutants but was lost in the *ΔpetB* strain that lacks cyt b_6 (apocytochrome b_6 24 kD), where CCB1 migrated only as a monomer of ~45 kD of apparent molecular mass. Interestingly, an oligomeric form of cyt b_6, which was visible in the same 70–110-kD region in the WT and in *petB-C35V*, *ccb2*, *ccb4*, and *ccb3* mutants, was depleted in the *ccb1* mutant. These migration patterns support the existence of a CCB1/b_6 oligomer. Oligomeric forms of CCB2, CCB3, and CCB4 at 170 kD disappear altogether in the *ccb2*, *ccb3*, and *ccb4* mutants. This behavior is consistent with their association in a 170-kD complex. This 170-kD oligomer is also absent in the *ΔpetB* mutant, an observation that is consistent with an interaction between the CCB2/CCB4/CCB3 oligomer and cyt b_6. We note that this complex is also absent in the *ccb1* mutant, although we found no evidence for the presence of CCB1 in the 170-kD region. Because formation of the CCB1/b_6 oligomer still occurs in the *ccb2*, *ccb3*, and *ccb4* mutants, we suggest that formation of the CCB1/b_6 oligomer is a prerequisite for the formation of the CCB2/CCB4/CCB3 oligomer in the process of c_i-heme binding to cyt b_6.

Interactions between the CCBs and cyt b_6, as analyzed by coimmunoprecipitation

To gather independent evidence for the association of several CCB factors in these oligomeric complexes, some of which likely contain cyt b_6, we undertook complementary coimmunoprecipitation assays using antibodies raised against CCB3 peptides

Published June 29, 2009

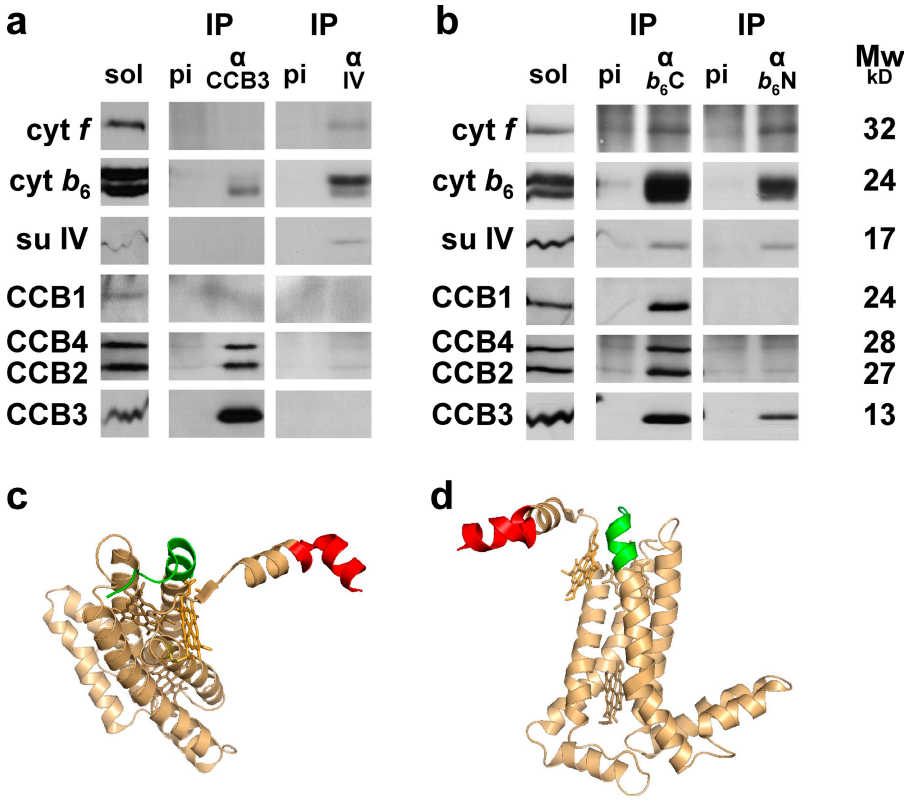

Figure 5. **Coimmunoprecipitation analysis of CCBs and cyt b_6 interactions.** Digitonin-solubilized membranes (prepared as for BN-PAGE) from the *petB-C35V* strain were incubated with protein A–Sepharose beads coupled to antibodies against peptides of CCB3 (α-CCB3), subunit IV N terminus (α-IV), cyt b_6 C terminus (α-b_6C), and cyt b_6 N terminus (α-b_6N), or against respective preimmune serum (pi). (a) Coimmunoprecipitations with α-CCB3 and α-IV. (b) Coimmunoprecipitations with α-b_6C and α-b_6N. Aliquots of digitonin-solubilized membranes (sol) and immunoprecipitates (IP) were separated by SDS-PAGE and analyzed by immunoblotting. (c) Top view from the *n* side of the membrane and (d) side view in the membrane plane of the cyt b_6 structure. Images in c and d were generated using PyMol and the coordinates from pdb file 1Q90 with α-b_6N peptide antigen in red, α-b_6C peptide antigen in green, b_L and b_H-hemes in brown, c_i-heme in orange, and Cys35 in yellow.

(α-CCB3), the N-terminal domain of subunit IV (α-IV), and the N-terminal (α-b_6N) and C-terminal domains (α-b_6C) of cyt b_6 (Fig. 5). These antibodies detect the proteins against which they were prepared and not the other b_6f subunits or CCBs (controls not depicted). We used digitonin-solubilized membranes (as prepared for BN-PAGE) from the *petB-C35V* strain, as it shows the most abundant CCB oligomeric complexes in BN-PAGE. Coimmunoprecipitations were then assayed with polyclonal antibodies against peptides from cyt *f*, cyt b_6, subunit IV, CCB1, CCB2, CCB3, and CCB4.

Fig. 5 a shows that α-CCB3 coimmunoprecipitates CCB2, CCB4, and cyt b_6 but not CCB1, subunit IV, and cyt *f*. These results confirm that CCB3 indeed interacts with CCB2, CCB4, and cyt b_6, as suggested by the existence of the 170-kD oligomeric form of these three CCB components in BN-PAGE. That α-CCB3 pulls down cyt b_6 but not the other b_6f subunits and that α-IV pulls down b_6f subunits but no CCB components (Fig. 5 a) indicates that CCBs interact with cyt b_6 before its assembly within the b_6f complex.

Coimmunoprecipitations with α-b_6C and α-b_6N pulled down subunit IV and cyt *f* as expected from the formation of b_6f complexes in the *petB-C35V* mutant (see the following results section). In addition, α-b_6C coimmunoprecipitated the four CCBs, whereas α-b_6N coimmunoprecipitated only CCB3 out of the four CCBs (Fig. 5 b). These results support the interaction of the CCB2/CCB4/CCB3 oligomer with cyt b_6, as suggested by our BN-PAGE study. They also confirm the formation of CCB1/b_6 and CCB3/b_6 complexes. When using WT membranes, α-b_6N and α-b_6C coimmunoprecipitated subunit IV and cyt *f* but little if any CCBs (unpublished data), which is consistent with the low amount of CCB hetero-oligomers interacting with cyt b_6, as detected in BN-PAGE experiments in the WT.

The difference between α-b_6C, which coimmunoprecipitates the four CCBs, and α-b_6N, which selectively coimmunoprecipitates CCB3, suggests that the binding site of α-b_6N on cyt b_6 is masked whenever this cyt interacts with CCB1 or CCB2/CCB4/CCB3, thereby preventing α-b_6N access to its epitope. This steric constraint is consistent with the folding of polypeptide chains around the Q_i site in the vicinity of the c_i-heme–binding site, as revealed by the three-dimensional structure of b_6f complexes. Indeed, a heme ligation complex is expected to interact with cyt b_6 on the stromal end of its first transmembrane helix in order to covalently attach c_i-heme by a thioether bond to Cys35 (Fig. 5, c and d). In the b_6f complex structure (Stroebel et al., 2003), the N terminus of cyt b_6 forms an amphipathic helix lying parallel to the membrane plane on the stromal face of the membrane near the quinone binding site Q_i. The Q_i site opens onto the hydrophobic groove at the dimer interface.

α-b_6C coimmunoprecipitation before BN-PAGE depleted the digitonin extract in most of the CCB2/CCB4/CCB3-containing complex at 170 kD as well as in the CCB1-containing complexes found in the 70–110-kD region. In contrast, it did not modify the level of CCB2/CCB4-containing oligomers of 70 kD. These results confirm that cyt b_6 is associated with the two oligomeric complexes of higher molecular mass but not with the CCB2/CCB4 heterodimer (Fig. 6).

To identify heme-containing intermediates among the CCBs, we attempted to detect peroxidase activity caused by covalent heme binding on these proteins after SDS-PAGE. We used the whole membrane fraction as well as digitonin-solubilized membranes followed by α-b_6C coimmunoprecipitation from the *petB-C35V* strain, which accumulates assembly intermediates. We failed to detect any sign of peroxidase activity in either case.

Published June 29, 2009

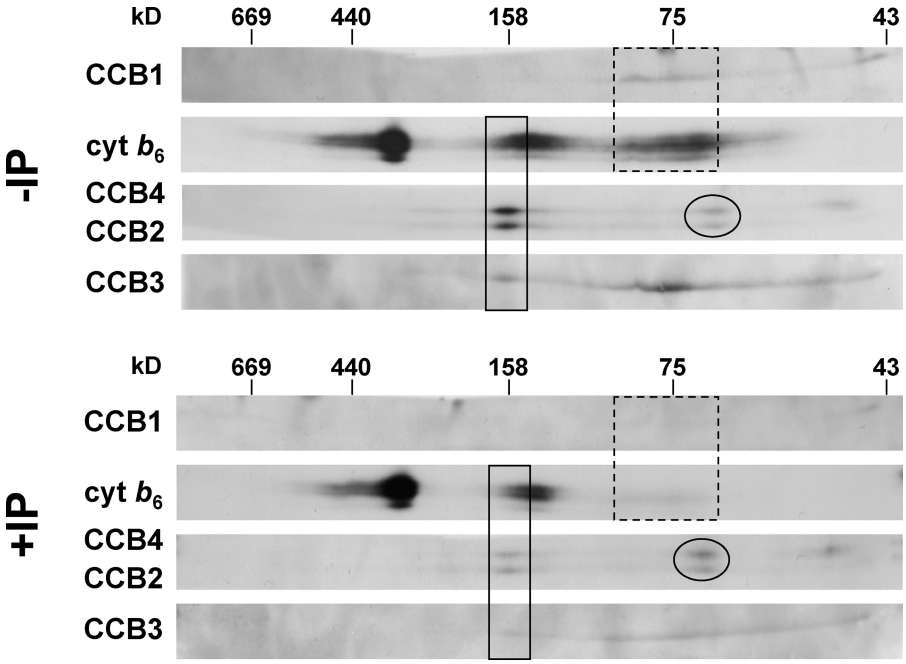

Figure 6. **CCB complex depletion by α-b_6C coimmunoprecipitation in BN-PAGE.** Half of the digitonin-solubilized membranes from the *petB-C35V* strain were incubated with protein A–Sepharose beads coupled to antibodies against a peptide of cyt b_6 C terminus (α-b_6C). Digitonin-solubilized proteins without immunoprecipitation (−IP) and of the unbound fraction after α-b_6C immunoprecipitation (+IP) were separated in the first dimension by the same BN-PAGE and in the second dimension by SDS-PAGE, and analyzed by ECL immunodetection. CCB2/CCB4/CCB3/b_6 (solid boxes), CCB1/b_6 (dashed boxes), and CCB2/CCB4 heterodimer (circles) are indicated.

It is of note that we were able to detect peroxidase activity of 1% but not of 0.1% of cyt *f* using serial dilutions of SDS-solubilized WT membranes (Fig. S1). Thus, assuming that the mRNA ratios would reflect protein ratios for nucleus-encoded products (i.e., 70-fold less mRNA accumulation for *CCB* genes than for nuclear genes encoding b_6f complex subunits; Karpowicz, S., and S. Merchant, personal communication) and that assembly intermediates recruit most of the CCBs, we would tentatively conclude the absence of covalent heme binding to any of the CCBs.

b_6f complex assembles in the absence of c_i-heme binding but is highly protease sensitive

By BN-PAGE, we could also investigate the state of b_6f complex assembly (Fig. 7 a). In the WT, dimers and monomers of b_6f complex were easily detected by comigration of cyt *f*, cyt b_6, and subunit IV at 320 kD and 140 kD, respectively (Fig. 7 a), which is in agreement with previous studies (Breyton et al., 1997; Lennartz et al., 2006). Despite the low abundance of b_6f subunits in the *petB-C35V* strain, as well as in all *ccb* mutant strains (see cyt b_6 in Fig. 4, other b_6f subunits not shown), dimeric and monomeric forms of b_6f complex could still be detected, which indicates that covalent binding of the c_i-heme is not a prerequisite for assembly of cyt b_6 within b_6f complexes. However, the low accumulation of the b_6f complex in *petB-C35V* and *ccb* mutant strains (Kuras et al., 1997; de Vitry et al., 2004) suggests that c_i-heme binding contributes to the folding of b_6f complexes in a protease-resistant form. This lower accumulation is not visible in Fig. 4 and Fig. 7 a because we overexposed the immunoblots for the b_6f subunits in the *ccb* and *petB-C35V* mutants, as compared with that in the WT (exposure time of 2 min instead of 20 s). In contrast, the assembly of b_6f complex was totally impaired in substitution mutants lacking either one of the four conserved histidines in the sequence of cyt b_6, which are axial ligands of b_H- or b_L-hemes (Fig. 7 a).

We wondered whether these assembled forms of b_6f complex retained any functional properties. To this end, we closely examined the fluorescence induction patterns in vivo of *ccb* and *petB-C35V* mutants. In vivo fluorescence induction kinetics were measured using low actinic light followed by a saturating pulse to determine F_{max}. As shown in Fig. 7 b, the stationary fluorescence in the *petB-C35V* strain was higher than in the WT but remained well below F_{max} in these experimental conditions. Similar fluorescence data were obtained with the four *ccb* strains (not depicted). In contrast, both the *ΔpetB* strain (Fig. 7 b) and the substitution mutants of the axial ligands of b_H- and b_L-hemes (not depicted) showed a stationary fluorescence very close to F_{max}, as expected from the block in electron transfer between PSII and PSI. These results indicate that the plastoquinone pool is not fully reduced in the stationary state in *petB-C35V* and *ccb* strains under our light intensity conditions. Thus, the low amount of assembled b_6f complex lacking covalent binding of the c_i-heme contributes to some reoxidation of the plastoquinol pool at low light intensity.

Discussion

Polytopic transmembrane topologies of CCB1–4

The CCBs are required for covalent attachment of c_i-heme to cyt b_6 in the thylakoid membrane. These proteins are encoded by the nuclear genome, translated as precursors with N-terminal transit peptides to the chloroplast, where they are inserted within membranes (Kuras et al., 2007; Lezhneva et al., 2008). Based on the analysis of the CCB sequences, we previously proposed that CCB1–4 proteins had a similar topology in *C. reinhardtii* (Kuras et al., 2007) and in *A. thaliana* (Lezhneva et al., 2008). Our protein folding model (Kuras et al., 2007) took into account the prediction of TMDs using multiple sequence alignments (TMAP; Persson and Argos, 1994) and the prediction of the

Published June 29, 2009

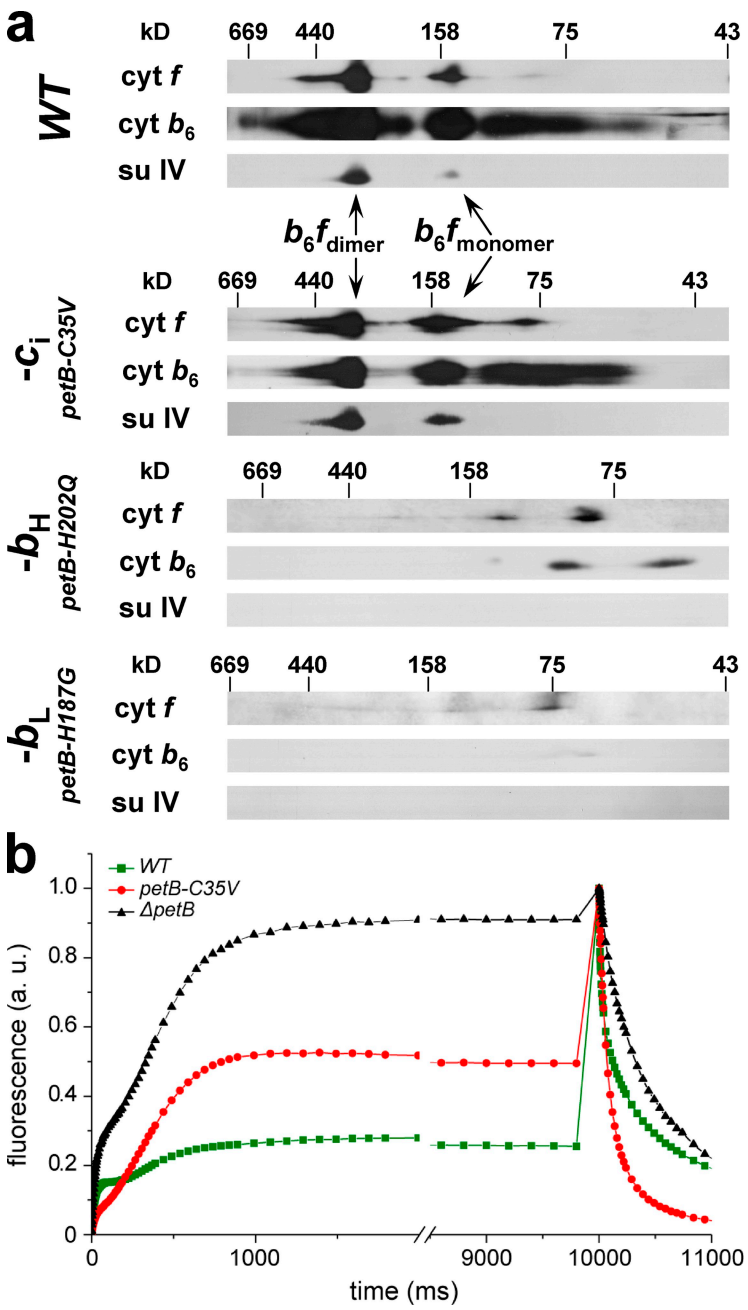

Figure 7. **Analysis of b_6f complex assembly in BN-PAGE and activity in vivo.** (a) b_6f complexes after BN-PAGE of digitonin-solubilized membranes. Shown are a WT strain, *petB-C35V* (-c_i) strain, and *petB-H202Q* (-b_H) strain: a site-directed mutant of the chloroplast *petB* gene with a substitution of His202 involved as an axial ligand of b_H-heme preventing b_H-heme binding to cyt b_6. *petB-H187G* (-b_L) strain: site-directed mutant of the chloroplast *petB* with a substitution of His187 involved as axial ligand of b_L-heme preventing b_L-heme binding to cyt b_6. Digitonin-solubilized proteins were separated in the first dimension by BN-PAGE and in the second dimension by SDS-PAGE and analyzed by ECL immunodetection. b_6f complex migrates as a dimer of 320 kD (b_6f_{dimer}) and as a monomer of 140 kD ($b_6f_{monomer}$), both highlighted by arrows. (b) Fluorescence induction kinetics of dark-adapted cells from *WT*, *petB-C35V*, and *ΔpetB* strains.

localization of positively charged segments by the "positive inside rule" at the borders of the putative TMDs (Gavel et al., 1991). This transmembrane organization is supported here by our biochemical study, based on chaotropic extraction, protease accessibility, and split ubiquitin data (Fig. 1 c). In particular, the high protease sensitivity in the absence of vesicle sonication of the two homologues CCB2 and CCB4 is easily explained by their large C-terminal domains exposed to the stromal side of the membranes. Split ubiquitin experiments are consistent with a localization of N and C termini of CCB2 and CCB4 in the yeast cytosol (the compartment corresponding to the chloroplast stroma), thereby confirming our folding model with two TMDs. CCB1 is degraded at a higher trypsin concentration than CCB2 and CCB4, as expected for a protein with three TMDs and short stromal exposed domains. Split ubiquitin experiments further support the localization of the C terminus of CCB1 in the cytosol. CCB3 is very resistant to trypsin treatments, as expected for a hydrophobic protein with two TMDs and short N and C termini exposed to the lumen. That we did not detect a CCB3 digestion product corresponding to the mature protein missing the three C-terminal amino acid residues further supports the lumenal localization of the C terminus of CCB3.

CCB2 and CCB4 form a stable heterodimer

This study provides extensive evidence for the association of CCB2 and CCB4 in a stable heterodimer in vivo. They accumulate in a concerted manner in *C. reinhardtii* and they interact in two hybrid experiments. Moreover BN-PAGE showed that they are part of a 70-kD complex in all *C. reinhardtii* strains we examined,

Published June 29, 2009

except for *ccb2* and *ccb4* mutants, which lack these two proteins. CCB2 and CCB4 are derived from a unique cyanobacterial ancestor likely duplicated upon endosymbiosis (Kuras et al., 2007). It is likely that cyanobacteria contain a CCB2/4-like homodimer. The molecular information born by a single CCB2/4-like protein in cyanobacteria is split between the eukaryotic CCB2 (about 30 residues after the second TMD) and CCB4 (mainly in the protein C terminus) with little redundancy (Fig. S2), which further substantiates the need for heterodimer formation in the latter case. The photosynthesis apparatus offers two other remarkable examples of heterodimer formation between two homologous proteins: the two core proteins of PSII (D1 and D2) and the two core subunits of PSI (PsaA and PsaB). In the case of type I reaction centers, a homodimer of pshA, still found in some bacteria like heliobacteria, is reminiscent of the ancestral PSI (for review see Heinnickel and Golbeck, 2007).

Distinct CCB hetero-oligomers interact with cyt b_6

The presence or absence of cyt b_6 had no influence on the accumulation level of any of the CCBs. However, based on BN-PAGE and coimmunoprecipitation experiments, we could identify several hetero-oligomers that interact with cyt b_6: a CCB1/b_6 complex of ~70-110 kD and a CCB2/CCB4/CCB3 protein complex of 170 kD in BN-PAGE, the existence of which are confirmed by their coimmunoprecipitation with cyt b_6. The accumulation of these protein complexes is particularly visible in the *petB-C35V* strain. Therefore, we consider that these CCB/b_6 hetero-oligomers are transiently formed in the process of heme delivery to the cyt b_6 substrate and are trapped in the *petB-C35V* mutant, which contains the same CCB protein complement as in the WT but is blocked at the very last step of c_i-heme binding to cyt b_6. We noted that α-b_6C coimmunoprecipitates the four CCBs, whereas α-b_6N selectively coimmunoprecipitates CCB3. Collectively, these observations argue for the formation of an additional CCB3/b_6 complex, distinct from CCB1/b_6 and CCB2/CCB4/CCB3/b_6 complexes, a conclusion further supported in BN-PAGE by the shift to a lower apparent molecular mass of the CCB3-containing band in the *ΔpetB* strain. The b_6f monomer and dimer were estimated to contain ~60% protein and prosthetic groups and 40% detergents and lipids (Breyton et al., 1997). Assuming (1) the same protein to lipid/detergent ratio in each CCB-containing oligomer and (2) that they would contain only one copy of their constitutive subunits, the 170-kD CCB2/CCB4/CCB3/b_6 oligomer would have a calculated mass of 155 kD (protein mass of 93 kD), and the 70–110-kD CCB1/b_6 oligomer would have a calculated mass of 82 kD (protein mass of 49 kD). Although these calculated values compare well with those from BN-PAGE, we cannot exclude that these three hetero-oligomers would contain additional protein subunits, as yet unknown CCB factors, or several copies of some of their subunits.

Tentative model for a CCB-mediated apo- to holo-cyt b_6 conversion

Transient and stable complexes are required for cyt *c* biogenesis on the *p* side of membranes. In bacterial/mitochondrial system I, cyt *c* maturation E (CcmE) binds heme covalently (Schulz et al., 1998) upon interaction with CcmC and CcmD (Ren et al., 2002; Ahuja and Thöny-Meyer, 2005). Holo-CcmE is then released by the CcmA/CcmB ABC transporter (Christensen et al., 2007; Rayapuram et al., 2007). CcmE then interacts with CcmF and CcmH to perform heme ligation to the apocytochrome (Ren et al., 2002; Meyer et al., 2005; Rayapuram et al., 2008; Sanders et al., 2008). In bacterial–cyanobacterial–chloroplast system II, CCSA and CCS1 are part of a 200-kD heme delivery complex (Dreyfuss et al., 2003; Hamel et al., 2003). In mitochondrial system III, cyt *c* and c_1-heme lyases have been identified, and interactions between heme lyase and apocytochrome *c* have been demonstrated (Mayer et al., 1995).

We expect that system IV, composed of CCBs, should have features distinct from the three other systems because it develops on the opposite side of the membranes. Furthermore, the ferrochelatase produces the heme and the c_i-heme–binding site, with both on the stromal side of the membrane, and we do not expect the need for a transmembrane protein that would translocate the heme from one side of the membrane to the other, as it must occur for cyt biogenesis systems on the *p* side of the membranes. For example, the CCSA–CCS1 complex is believed to perform this initial step before heme binding on the apocytochrome. Indeed, the experimentally tested transmembrane topologies of CCB1–4 protein confirm that most of the conserved tryptophane and/or tyrosine residues that are expected to interact with heme from what is currently known in other maturation systems are all located on the *n* side of the thylakoid membranes. These conserved residues might participate in heme chaperoning and delivery to cyt b_6 on the stromal side of the membranes. We also note that none of the four CCB factors has conserved cysteine residues, which are critical for apocytochrome and/or heme reduction in system I–II, as exemplified by the membrane-anchored thioredoxin-like protein HCF164 (Lennartz et al., 2001; Motohashi and Hisabori, 2006) that would interact with the transmembrane protein CCDA (Page et al., 2004) as a redox relay component required for reduction of the two cysteines at the heme-binding site of apocytochromes *f* and c_6. We cannot exclude that it is merely due to the existence of additional protein factors that have escaped our genetic screen. However, one should consider the possible absence of catalytic cysteines in the process of heme binding on the *n* side of membranes because of numerous chemical species that have the potential to maintain the protein thiols in the stroma and cyanobacterial cytoplasm, such as the presence of thioredoxins that maintain largely reduced cysteine residues (for review see Herrmann et al., 2009). We cannot exclude either an unusual heme-binding process by a unique thioether bond or the easier access of heme-delivery complexes to the ferrous heme produced by the neighboring ferrochelatase (van Lis et al., 2005). However, none of the four CCBs displays a conserved histidine residue, which is involved in covalent heme binding to CcmE in system I (Schulz et al., 1998). Collectively with our inability to detect any peroxidase activity associated with the CCBs, this argues for the absence of a CCB intermediate carrying a covalently bound heme.

The various CCB-containing complexes that we identified in *C. reinhardtii* have given us access to some supramolecular traits of the biogenesis pathway for cyt b_6 on the *n* side of membranes.

Published June 29, 2009

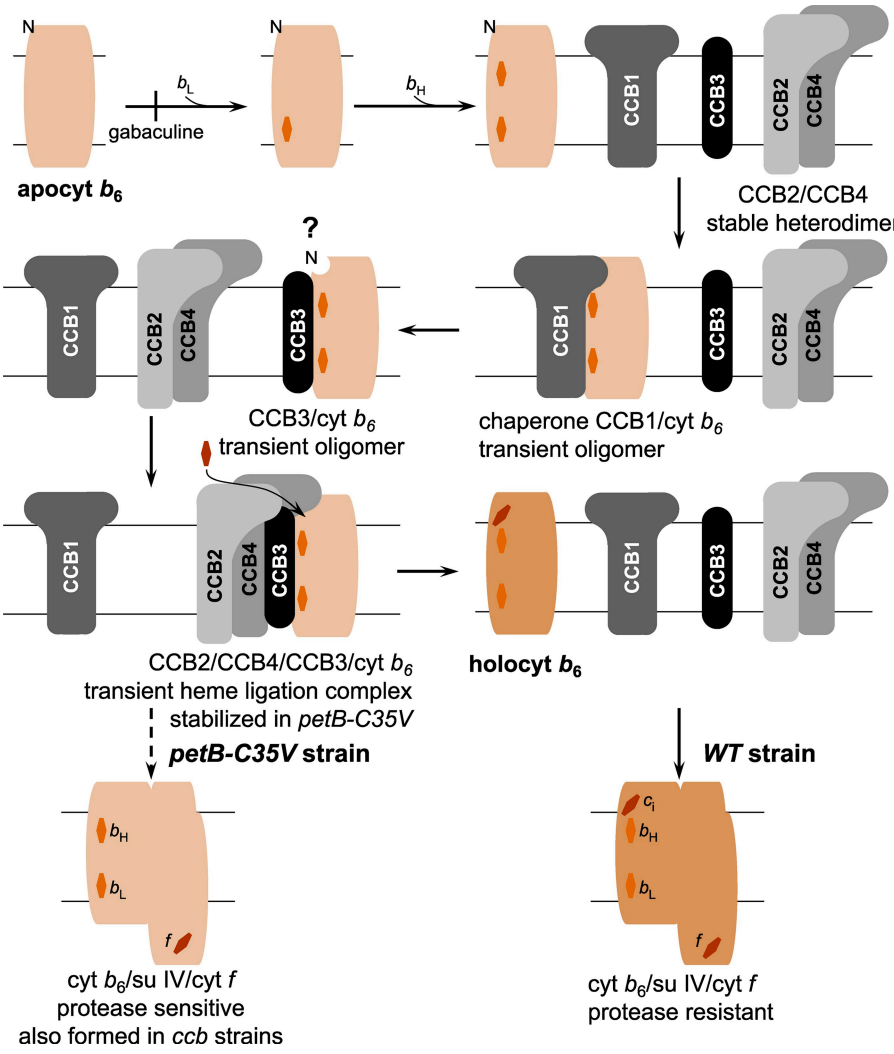

Figure 8. **Tentative model for a CCB-mediated apo- to holo-cyt b_6 conversion.** Model with the following steps: membrane integration of apocyt b_6, formation of a b_L-heme–dependent intermediate that can be prevented by heme depletion (gabaculine treatment), and formation of a b_L and b_H binding cyt b_6 (Kuras et al., 1997); formation of a transient oligomer comprising CCB1/b_6, formation of a transient oligomer comprising CCB3/b_6, association of the oligomer comprising CCB3/b_6 with the stable heterodimer CCB2/CCB4 to form the heme ligation complex, and a transient oligomer comprising CCB2/4/3/b_6, which is stabilized in *petB-C35V* strain; c_i binding leads to a holocyt b_6 with three hemes; and cyt b_6 associates with other b_6f subunits even in the absence of c_i-heme covalent binding. The binding site of α-b_6N on cyt b_6 (N) is masked whenever this cyt interacts with CCB1 or CCB2/CCB4/CCB3, thereby preventing α-b_6N access to its epitope. The question mark indicates that CCB3/b_6 is a transient protein complex that may arise before formation or after dissociation of the CCB2/CCB4/CCB3/b_6 complex.

First, covalent binding of the c_i-heme to cyt b_6 occurs independently of its assembly within the b_6f complex. This is demonstrated by the diffuse aspect of the electrophoretic band for cyt b_6 in deletion mutants lacking other b_6f subunits, which is diagnostic of c_i-heme binding, instead of a double band in the absence of heme binding (Kuras et al., 1997). This is further supported by direct evidence for an interaction of cyt b_6 with CCB components, with the observation of a 70–110-kD CCB1/b_6 complex in BN-PAGE at much lower apparent molecular masses than assembled forms of b_6f complexes. The fact that interactions between cyt b_6 and the CCBs occur before its assembly within b_6f complexes is demonstrated by our coimmunoprecipitation experiments in which α-CCB3 pulls down only cyt b_6 among b_6f subunits, whereas α-IV did not pull down any CCB. That unassembled cyt b_6 but not the subunit IV–cyt b_6 complex is the substrate for the CCB machinery is consistent with the view that a split cyt *b* would be a prerequisite for c_i-heme insertion (Stroebel et al., 2003).

The full maturation of cyt b_6 through the CCB-heme–delivering pathway is not required for its assembly within b_6f complexes, as we detected both monomeric and dimeric forms of the protein complex in the absence of c_i-heme binding. A similar observation was recently reported for a *ccb2* mutant in *A. thaliana*. This mutant had a high chlorophyll fluorescence phenotype and showed no evidence for photosynthetic electron transport (Lyska et al., 2007). This is in contrast to our observation that the c_i-heme–binding defective strains in *C. reinhardtii* retain some activity in plastoquinol oxidation, as suggested by their fluorescence properties when illuminated at low light intensity. However, this activity in plastoquinol oxidation did not allow phototrophic growth in standard conditions (growth medium lacking reduced carbon sources, light intensities of 40–100 μE/m^2/s, ambient air and room temperature), which allowed us to recover the *CCB* genes by complementation with a selection scheme based on the restoration of phototrophy (Kuras et al., 2007).

That b_6f complexes can assemble in the absence of c_i-heme binding is in marked contrast to the required coordination of hemes b_H and b_L for cyt b_6 assembly within b_6f complexes, as shown by our comparative BN-PAGE experiments. As we observed b_6f complex assembly in each *ccb* mutant, we can exclude that either of these CCBs is required for the formation of an assembly competent form of a *b*-heme–containing cyt b_6.

On the basis of heme depletion upon gabaculine treatment and after analysis of mutants lacking axial ligands of b_L-heme or b_H-heme, we previously proposed that formation of a b_L-heme–dependent intermediate can be prevented by gabaculine treatment

Published June 29, 2009

(Kuras et al., 1997). Our sequential model for b_L integration as a prerequisite for b_H integration within apocytochrome b_6 has recently been supported by heterologous expression studies of mutant variants of cyt b_6 in *Escherichia coli* (Dreher et al., 2008). The biochemical data gathered in the present study allowed us to further enrich our original model for cyt b_6 maturation (Kuras et al. 1997), with sequential binding of b_L-heme, b_H-heme, and c_i-heme before assembly with other b_6f subunits (Fig. 8). In *ccb* and *petB-C35V* mutants, assembly of the b_6f complex continues despite the absence of covalent binding of c_i-heme. The resulting complex shows limited accumulation in the thylakoid membranes, probably because it displays an increased protease sensitivity.

In our model for a CCB-mediated apo- to holo-cyt b_6 conversion (Fig. 8), formation of a transient CCB1/b_6 oligomer that suggests a role of CCB1 in cyt b_6 chaperoning is followed by formation of a transient CCB3/b_6 oligomer. The latter then recruits the stable CCB2/CCB4 heterodimer to form the membrane-integral multisubunit heme ligation complex comprised of CCB2, CCB4, and CCB3, interacting with the cyt b_6. Whether CCB3/b_6 is an intermediate before formation (as shown in Fig. 8) or after dissociation of CCB2/CCB4/CCB3/b_6 complex is still an open question; indeed, CCB3 is mainly monomeric in the *ΔpetB* mutant but surprisingly still oligomerizes in *ccb1*, *ccb2*, and *ccb4* mutants. Concerning the specific roles of CCB2 and CCB4, one could speculate that CCB2, the less conserved CCB protein, would have evolved to adapt for heme scavenging in different organisms performing oxygenic photosynthesis, whereas the better conserved CCB4 protein would pack closely with CCB3 and cyt b_6, whose sequences are also well conserved. The binding of *b*-hemes to apocytochrome b_6 before c_i-heme binding makes it difficult to assess unambiguously the possible association of a heme with the CCB moiety of these transient oligomers. Once c_i-heme is thioether bound to Cys35 of cyt b_6, this membrane-integral multisubunit heme ligation complex dissociates, freeing CCB3 and the stable CCB2/CCB4 heterodimer, now available for a new round of catalysis.

The photosynthetic apparatus requires a diversity of biogenesis pathways for cofactor delivery to their protein substrates. With the present biochemical dissection of the CCB pathway, we now have a refined view of the protein scaffold involved in heme delivery to the photosynthetic membranes. In that respect, it is of note that the two machineries for heme delivery on the stromal and lumenal side of the membranes appear not to share any common protein components: mutants defective for the CCS pathway (heme binding on the lumenal side) showed unaltered heme binding to cyt b_6, and, similarly, CCB mutants show unaltered heme binding to cyt *f* (Kuras et al., 2007). How neosynthesized heme is distributed between these two pathways remains to be explored.

Materials and methods

Strains and culture conditions

C. reinhardtii mutants have been described previously and were as follows: *ccb*, *petB-C35V*, *petB-H202Q*, *petB-H137G*, and *ΔpetB* (Kuras et al., 1997, 2007; de Vitry et al., 2004). Cells were grown at 25°C in Tris acetate phosphate (TAP) medium, pH 7.2, under dim light (6 $\mu E/m^2/s$) and collected during the exponential phase at 2×10^6 cells per milliliter.

Protein preparation and analysis

Cell preparation and chaotropic extractions of membrane proteins were performed as described previously (Breyton et al., 1994; de Vitry et al., 2004), except that supernatants from NaCl and NaI extractions were washed on microcon (YM-3; Millipore) in DTT-Na_2CO_3 0.1 M. For proteolysis experiments, French press–derived thylakoid membrane vesicles were prepared extemporaneously as in Chua and Bennoun (1975) but without protease inhibitors, and finally washed twice with 20 mM Tris-HCl, pH 8.0. Various concentrations of trypsin were added to thylakoid membranes at a final chlorophyll concentration of 270 µg/ml. Half of each sample was sonicated three times for 10 s on ice. Trypsin treatments were performed at room temperature for 30 min, and the reaction was arrested by adding 2 mM phenyl methylsulfonylfluoride as an inhibitor. Polypeptides were separated on 12–18% SDS-polyacrylamide gels in the presence of 8 M urea (de Vitry et al., 1999). Proteins were electrotransferred onto Immobilon NC membranes (Westran S membranes; GE Healthcare) in a semidry blotting apparatus at 0.8 mA/cm^2 for 45 min. For immunodetection by the chemoluminescence method (GE Healthcare), we used antisera against cyt b_6, cyt *f*, subunit IV, PSII OEE subunits, and ATP synthase β subunit at a 1:10,000 dilution; CCB3 at a 1:2,500 dilution; and CCB1, CCB2, and CCB4 at a 1:300 dilution.

Yeast split ubiquitin two-hybrid assays

The principle is based on the in vivo split ubiquitin reconstitution caused by the strong interaction of the two ubiquitin moieties. The WT N-terminal half of ubiquitin (NubI) interacts with the C-terminal half of ubiquitin (Cub) even if these domains are fused to transmembrane proteins that do not interact; it is used as a positive control of transmembrane protein expression. Because the mutated N-terminal half of ubiquitin with a substituted isoleucine at position three for a glycine (NubG) has a lower affinity than NubI for Cub, it allows split ubiquitin reconstitution only when the two domains are fused to transmembrane proteins that interact. The transcription factor LexA-VP16 is fused to the Cub domain. Upon interaction of Cub and NubG or NubI, the polypeptide chain between Cub and LexA-VP16 is cleaved. It can translocate to the nucleus and activate transcription of genes, allowing growth in the absence of adenine or histidine or allowing β-galactosidase activity. The cleavage and translocation of the transcription factor require the two ubiquitin moieties located in the yeast cytoplasm. We used Alg5, a yeast transmembrane protein that is not expected to interact with our proteins of interest, fused to NubI as an expression control, or fused to NubG or Cub as an interaction test control. cDNA fragments coding for mature CCB1, CCB2, CCB4, and cyt b_6 were amplified by polymerase chain reaction (TripleMaster; Eppendorf) using primers listed in Table S1 that all contained a SfiI site used to fuse in frame the coding sequences to the ubiquitin NubG domain (pPR3-STE vector) and the ubiquitin Cub domain (pBT3-STE vector; DUALmembrane kit3; Dualsystems Biotech). The yeast NYM51 strain (Mata, leu2, trp1, his3, ade2, LYS2::$(lexAop)_4$-HIS3, ade2::$(lexAop)_8$-ADE2, ura3::$(lexAop)_8$-lacZ) was cotransformed with combinations of constructs expressing proteins fused to NubG and Cub domains. Cotransformants were allowed to grow for 3 d at 30°C on synthetic medium (SD) lacking leucine and tryptophan. The interaction between two proteins at the yeast membrane results in the activation of reporter genes *ADE2*, *HIS3*, and *lacZ*. The expression of auxotrophic growth markers *ADE2* and *HIS3* was monitored by the growth on a medium lacking adenine and histidine in the presence of 10 mM 3-aminotriazole. The expression of *lacZ* was followed by measuring at OD_{417nm} the accumulation of the product metabolized by β-galactosidase with 2.2 mM o-NPG (2-nitrophenyl β-D-galactopyranoside; Sigma-Aldrich) as a substrate (Rayapuram et al., 2008). A construct expressing Cub fused to the protein of the yeast endoplasmic reticulum Alg5 (pCCW-Alg5 vector) was used as negative control for the NubG fusions. In the same way, a construct expressing NubG fused to Alg5 (pDL2-Alg5 vector) was used as negative control for Cub fusions. Transformations in yeast were controlled by growth on a medium lacking both leucine and tryptophan.

BN-PAGE and immunoprecipitations

Membrane fractions were prepared from sonicated cell lysates as in Kuras et al., (2007). All steps up to the second dimension analysis were performed at 4°C. Membrane fraction was pelleted in a TLA-100.3 rotor (Beckmann Coulter) at 270,000 *g* for 10 min and resuspended in 50 mM Bis-Tris, pH 7.0, supplemented with 1× complete EDTA-free protease inhibitor mixture (Roche). Immediately after preparation, membranes were solubilized for 30 min in 50 mM Bis-Tris, pH 7.0, and 416 mM aminocaproic acid by 2.5% freshly prepared digitonin at a final concentration of chlorophyll of 0.75 mg/ml (corresponding to 6.68 g of detergent per gram of protein). Taurocholic acid (Sigma-Aldrich) was added to supernatant recovered after centrifugation in a TLA-100 rotor (Beckmann Coulter) at 250,000 *g* for

30 min, to a final concentration of 0.25% (wt/vol). Supernatant and molecular weight markers (gel filtration calibration kit HMW; GE Healthcare) in 50 mM Bis-Tris, pH 7.0, and 416 mM aminocaproic acid were loaded on a BN polyacrylamide gel (Schägger and von Jagow, 1991) with a 3% acrylamide stacking gel and a 6–18% acrylamide separating gel. Electrophoresis was initiated with cathode buffer containing 0.02% Coomassie blue for 1 h at 150 V, then overnight at 380 V. The buffer was then exchanged with new cathode buffer containing 0.002% Coomassie blue, and electrophoresis was continued for 6 h at 600 V. For the denaturizing second dimension analysis, strips cut out from the first BN gel were incubated at room temperature twice for 15 min in 1% SDS, 1 mM EDTA, 10 mM DTT, 100 mM Na_2CO_3, and protease inhibitors (200 µM phenylmethylsulfonyl fluoride, 1 mM benzamidine, and 5 mM aminocaproic acid), then washed five times for 5 min in 0.25 M Tris, 1.92 M glycine, 0.01% SDS, and 1 mM EDTA. The strips of BN-PAGE were then embedded in a stacking gel on top of a resolving 12–18% SDS-polyacrylamide gel containing 8 M urea, then electrotransferred and analyzed by immunoblotting. For immunoprecipitations, antibodies were coupled to protein A–Sepharose beads as in Schroda et al., (2001). The coupled beads were washed twice in 50 mM Bis-Tris, pH 7.0, 416 mM aminocaproic acid, and 0.2% digitonin, and incubated with digitonin-solubilized membranes (prepared as for BN-PAGE) for 1 h at 4°C. After immunoprecipitation, the coupled beads were washed three times in the previous solution and then twice in 10 mM Tris-HCl, pH 7.5. Immunoprecipitated proteins were recovered by resuspending the beads in 2% SDS and 12% sucrose and boiling for 50 s. After centrifugation, the supernatant was complemented to 0.1 M DTT and 0.1 M Na_2C0_3, and analyzed by SDS-PAGE. Peptide sequences recognized for immunoprecipitation and/or immunodetection experiments were SVTKKPDLSPDVLKY for α-IV (Pierre et al., 1995), SKVYDWFEERLEIQ for α-b_6N, and LMIRKQGISGPL for α-b_6C (de Vitry et al., 2004), which are localized in cyt b_6 structure in Fig. 5 (c and d); and RYYFKRYNYDVKETGE for α-CCB1, FSERPRALADRERGW for α-CCB2, GSCLAADSPENAEQTV and GPQGLLTLIQQRGGL for α-CCB3, and TVDFVEPGLKPYA for α-CCB4 (Kuras et al., 2007), which are localized in CCBs transmembrane topology in Fig. 1 c.

Biophysical measurements

Fluorescence kinetics were measured with a JTS10 spectrometer (Bio-Logic). Cells were dark-adapted for 1 min before each experiment. A low intensity (150 µE/m^2/s) continuous illumination was provided with an orange electroluminescent diode (620 nm), a light condition which generates a photosynthetic linear electron transfer of 100 electrons per second in the WT. A saturating pulse was added in the end of the low-light period to fully reduce the quinone pool. Fluorescence was detected with high-pass colored RG695 filters (Schott).

Online supplemental material

Fig. S1 shows the absence of detectable covalent heme binding on CCBs. Fig. S2 shows sequence alignments of CCB2 and CCB4 orthologues with conserved domains repartition highlighted, and schematizes their transmembrane topology. Table S1 describes primers, templates, and vectors used for split-ubiquitin experiments. Online supplemental material is available at http://www.jcb.org/cgi/content/full/jcb.200812025/DC1.

We acknowledge the advice of G. Bonnard and C. Raynaud for two-hybrid experiments, C. Breyton and O. Vallon for BN-PAGE, D. Drapier for immunoprecipitation, J. Alric for fluorescence, and Y. Choquet, X. Johnson and R. Kuras for critical reading of the manuscript.

This work was supported by Centre National de la Recherche Scientifique/Université Pierre et Marie Curie (UMR 7141) and Agence Nationale de la Recherche (ANR-07-BLAN-0114). D. Saint-Marcoux was supported by a Ministère de l'Enseignement Supérieur et de la Recherch fellowship and is attaché temporaire d'enseignement et de recherche at Université Pierre et Marie Curie Paris 06.

Submitted: 4 December 2008
Accepted: 28 May 2009

References

Ahuja, U., and L. Thöny-Meyer. 2005. CcmD is involved in complex formation between CcmC and the heme chaperone CcmE during cytochrome *c* maturation. *J. Biol. Chem.* 280:236–243.

Allen, J.W., A.P. Jackson, D.J. Rigden, A.C. Willis, S.J. Ferguson, and M.L. Ginger. 2008. Order within a mosaic distribution of mitochondrial *c*-type cytochrome biogenesis systems? *FEBS J.* 275:2385–2402.

Breyton, C., C. de Vitry, and J.L. Popot. 1994. Membrane association of cytochrome b_6f subunits. The Rieske iron-sulfur protein from *Chlamydomonas reinhardtii* is an extrinsic protein. *J. Biol. Chem.* 269:7597–7602.

Breyton, C., C. Tribet, J. Olive, J.P. Dubacq, and J.L. Popot. 1997. Dimer to monomer conversion of the cytochrome b_6f complex. Causes and consequences. *J. Biol. Chem.* 272:21892–21900.

Christensen, O., E.M. Harvat, L. Thöny-Meyer, S.J. Ferguson, and J.M. Stevens. 2007. Loss of ATP hydrolysis activity by CcmAB results in loss of *c*-type cytochrome synthesis and incomplete processing of CcmE. *FEBS J.* 274:2322–2332.

Chua, N.H., and P. Bennoun. 1975. Thylakoid membrane polypeptides of *Chlamydomonas reinhardtii*: wild-type and mutant strains deficient in photosystem II reaction center. *Proc. Natl. Acad. Sci. USA.* 72:2175–2179.

de Vitry, C., G. Finazzi, F. Baymann, and T. Kallas. 1999. Analysis of the nucleus-encoded and chloroplast-targeted rieske protein by classic and site-directed mutagenesis of *Chlamydomonas. Plant Cell.* 11:2031–2044.

de Vitry, C., A. Desbois, V. Redeker, F. Zito, and F.A. Wollman. 2004. Biochemical and spectroscopic characterization of the covalent binding of heme to cytochrome b_6. *Biochemistry.* 43:3956–3968.

Dreher, C., A. Prodohl, R. Hielscher, P. Hellwig, and D. Schneider. 2008. Multiple step assembly of the transmembrane cytochrome b_6. *J. Mol. Biol.* 382:1057–1065.

Dreyfuss, B.W., P.P. Hamel, S.S. Nakamoto, and S. Merchant. 2003. Functional analysis of a divergent system II protein, Ccs1, involved in *c*-type cytochrome biogenesis. *J. Biol. Chem.* 278:2604–2613.

Ferguson, S.J., J.M. Stevens, J.W. Allen, and I.B. Robertson. 2008. Cytochrome *c* assembly: a tale of ever increasing variation and mystery? *Biochim. Biophys. Acta.* 1777:980–984.

Gavel, Y., J. Steppuhn, R. Herrmann, and G. von Heijne. 1991. The 'positive-inside rule' applies to thylakoid membrane proteins. *FEBS Lett.* 282:41–46.

Giege, P., J.M. Grienenberger, and G. Bonnard. 2008. Cytochrome *c* biogenesis in mitochondria. *Mitochondrion.* 8:61–73.

Gumpel, N.J., L. Ralley, J. Girard-Bascou, F.A. Wollman, J.H. Nugent, and S. Purton. 1995. Nuclear mutants of *Chlamydomonas reinhardtii* defective in the biogenesis of the cytochrome b_6f complex. *Plant Mol. Biol.* 29:921–932.

Hamel, P., V. Corvest, P. Giegé, and G. Bonnard. 2009. Biochemical requirements for the maturation of mitochondrial *c*-type cytochromes. *Biochim. Biophys. Acta.* 1793:125–138.

Hamel, P.P., B.W. Dreyfuss, Z. Xie, S.T. Gabilly, and S. Merchant. 2003. Essential histidine and tryptophan residues in CcsA, a system II polytopic cytochrome *c* biogenesis protein. *J. Biol. Chem.* 278:2593–2603.

Heinnickel, M., and J.H. Golbeck. 2007. Heliobacterial photosynthesis. *Photosynth. Res.* 92:35–53.

Herrmann, J.M., F. Kauff, and H.E. Neuhaus. 2009. Thiol oxidation in bacteria, mitochondria and chloroplasts: Common principles but three unrelated machineries? *Biochim. Biophys. Acta.* 1793:71–77.

Inoue, K., B.W. Dreyfuss, K.L. Kindle, D.B. Stern, S. Merchant, and O.A. Sodeinde. 1997. Ccs1, a nuclear gene required for the post-translational assembly of chloroplast *c*-type cytochromes. *J. Biol. Chem.* 272:31747–31754.

Kranz, R., R. Lill, B. Goldman, G. Bonnard, and S. Merchant. 1998. Molecular mechanisms of cytochrome *c* biogenesis: three distinct systems. *Mol. Microbiol.* 29:383–396.

Kuras, R., C. de Vitry, Y. Choquet, J. Girard-Bascou, D. Culler, S. Buschlen, S. Merchant, and F.A. Wollman. 1997. Molecular genetic identification of a pathway for heme binding to cytochrome b_6. *J. Biol. Chem.* 272:32427–32435.

Kuras, R., D. Saint-Marcoux, F.A. Wollman, and C. de Vitry. 2007. A specific *c*-type cytochrome maturation system is required for oxygenic photosynthesis. *Proc. Natl. Acad. Sci. USA.* 104:9906–9910.

Kurisu, G., H. Zhang, J.L. Smith, and W.A. Cramer. 2003. Structure of the cytochrome b_6f complex of oxygenic photosynthesis: tuning the cavity. *Science.* 302:1009–1014.

Lennartz, K., H. Plucken, A. Seidler, P. Westhoff, N. Bechtold, and K. Meierhoff. 2001. HCF164 encodes a thioredoxin-like protein involved in the biogenesis of the cytochrome b_6f complex in *Arabidopsis. Plant Cell.* 13:2539–2551.

Lennartz, K., S. Bossmann, P. Westhoff, N. Bechtold, and K. Meierhoff. 2006. HCF153, a novel nuclear-encoded factor necessary during a post-translational step in biogenesis of the cytochrome *bf* complex. *Plant J.* 45:101–112.

Lezhneva, L., R. Kuras, G. Ephritikhine, and C. de Vitry. 2008. A novel pathway of cytochrome *c* biogenesis is involved in the assembly of the cytochrome b_6f complex in *Arabidopsis* chloroplasts. *J. Biol. Chem.* 283:24608–24616.

Lyska, D., S. Paradies, K. Meierhoff, and P. Westhoff. 2007. HCF208, a homolog of *Chlamydomonas* CCB2, is required for accumulation of native cytochrome b_6 in *Arabidopsis thaliana. Plant Cell Physiol.* 48:1737–1746.

Mayer, A., W. Neupert, and R. Lill. 1995. Translocation of apocytochrome *c* across the outer membrane of mitochondria. *J. Biol. Chem.* 270:12390–12397.

Meyer, E.H., P. Giege, E. Gelhaye, N. Rayapuram, U. Ahuja, L. Thöny-Meyer, J.M. Grienenberger, and G. Bonnard. 2005. AtCCMH, an essential component of the *c*-type cytochrome maturation pathway in *Arabidopsis* mitochondria, interacts with apocytochrome *c*. *Proc. Natl. Acad. Sci. USA.* 102:16113–16118.

Motohashi, K., and T. Hisabori. 2006. HCF164 receives reducing equivalents from stromal thioredoxin across the thylakoid membrane and mediates reduction of target proteins in the thylakoid lumen. *J. Biol. Chem.* 281:35039–35047.

Page, M.L., P.P. Hamel, S.T. Gabilly, H. Zegzouti, J.V. Perea, J.M. Alonso, J.R. Ecker, S.M. Theg, S.K. Christensen, and S. Merchant. 2004. A homolog of prokaryotic thiol disulfide transporter CcdA is required for the assembly of the cytochrome b_6f complex in *Arabidopsis* chloroplasts. *J. Biol. Chem.* 279:32474–32482.

Pasch, J.C., J. Nickelsen, and D. Schunemann. 2005. The yeast split-ubiquitin system to study chloroplast membrane protein interactions. *Appl. Microbiol. Biotechnol.* 69:440–447.

Persson, B., and P. Argos. 1994. Prediction of transmembrane segments in proteins utilising multiple sequence alignments. *J. Mol. Biol.* 237:182–192.

Pierre, Y., C. Breyton, D. Kramer, and J.L. Popot. 1995. Purification and characterization of the cytochrome b_6f complex from *Chlamydomonas reinhardtii*. *J. Biol. Chem.* 270:29342–29349.

Rayapuram, N., J. Hagenmuller, J.M. Grienenberger, P. Giege, and G. Bonnard. 2007. AtCCMA interacts with AtCcmB to form a novel mitochondrial ABC transporter involved in cytochrome *c* maturation in *Arabidopsis*. *J. Biol. Chem.* 282:21015–21023.

Rayapuram, N., J. Hagenmuller, J.M. Grienenberger, G. Bonnard, and P. Giege. 2008. The three mitochondrial encoded CcmF proteinsform a complex that interacts with CcmH and *C*-type apo-cytochromes in *Arabidopsis*. *J. Biol. Chem.* 283:25200–25208.

Ren, Q., U. Ahuja, and L. Thöny-Meyer. 2002. A bacterial cytochrome *c* heme lyase. CcmF forms a complex with the heme chaperone CcmE and CcmH but not with apocytochrome *c*. *J. Biol. Chem.* 277:7657–7663.

Sanders, C., S. Turkarslan, D.W. Lee, O. Onder, R.G. Kranz, and F. Daldal. 2008. The cytochrome *c* maturation components CcmF, CcmH and CcmI form a membrane-integral multisubunit heme ligation complex. *J. Biol. Chem.* 283:29715–29722.

Schägger, H., and G. von Jagow. 1991. Blue native electrophoresis for isolation of membrane protein complexes in enzymatically active form. *Anal. Biochem.* 199:223–231.

Schroda, M., O. Vallon, J.P. Whitelegge, C.F. Beck, and F.A. Wollman. 2001. The chloroplastic GrpE homolog of *Chlamydomonas*: two isoforms generated by differential splicing. *Plant Cell.* 13:2823–2839.

Schulz, H., H. Hennecke, and L. Thöny-Meyer. 1998. Prototype of a heme chaperone essential for cytochrome *c* maturation. *Science.* 281:1197–1200.

Stroebel, D., Y. Choquet, J.L. Popot, and D. Picot. 2003. An atypical haem in the cytochrome b_6f complex. *Nature.* 426:413–418.

Thöny-Meyer, L. 2002. Cytochrome *c* maturation: a complex pathway for a simple task? *Biochem. Soc. Trans.* 30:633–638.

van Lis, R., A. Atteia, L.A. Nogaj, and S.I. Beale. 2005. Subcellular localization and light-regulated expression of protoporphyrinogen IX oxidase and ferrochelatase in *Chlamydomonas reinhardtii*. *Plant Physiol.* 139:1946–1958.

Xie, Z., and S. Merchant. 1996. The plastid-encoded *ccsA* gene is required for heme attachment to chloroplast *c*-type cytochromes. *J. Biol. Chem.* 271:4632–4639.